| | |
|---|---|
| Volume 1 | Grain Boundary Phenomena in Electronic Ceramics |
| Volume 2 | Physics of Fiber Optics |
| Volume 3 | Science and Technology of Zirconia |
| Volume 4 | Nucleation and Crystallization in Glasses |
| Volume 5 | Materials Processing in Space |
| Volume 6 | Character of Grain Boundaries |
| Volume 7 | Additives and Interfaces in Electronic Ceramics |
| Volume 8 | Nuclear Waste Management |
| Volume 9 | Forming of Ceramics |
| Volume 10 | Structure and Properties of MgO and $Al_2O_3$ Ceramics |
| Volume 11 | Processing for Improved Productivity |
| Volume 12 | Science and Technology of Zirconia II |
| Volume 13 | New Developments in Monolithic Refractories |
| Volume 14 | Ceramics in Heat Exchangers |
| Volume 15 | Fourth International Conference on Ferrites, Part I |
| Volume 16 | Fourth International Conference on Ferrites, Part II |
| Volume 17 | Fission-Product Behavior in Ceramic Oxide Fuel |
| Volume 18 | Commercial Glasses |
| Volume 19 | Multilayer Ceramic Devices |
| Volume 20 | Nuclear Waste Management II |
| Volume 21 | Ceramic Powder Science |
| Volume 22 | Fractography of Glasses and Ceramics |
| Volume 23 | Nonstoichiometric Compounds |
| Volume 24 | Science and Technology of Zirconia III |
| Volume 25 | Fabrication and Properties of Lithium Ceramics |
| Volume 26 | Ceramic Substrates and Packages for Electronic Applications |
| Volume 27 | Fabrication and Properties of Lithium Ceramics II |

ADVANCES IN CERAMICS • VOLUME 27

# FABRICATION AND PROPERTIES OF LITHIUM CERAMICS II

**Edited by**

**Glenn W. Hollenberg**
**Ian J. Hastings**

The American Ceramic Society, Inc.
Westerville, Ohio

HTO(g), or $T_2O$(g) from oxidic ceramic tritium breeders. The degree of surface coverage at a given time, the result of adsorption of $H_2O$ or $H_2$, and diffusion of T to the surface will determine which type of site is dominant in the release process and what the desorption activation energy will be at that time. Theoretical predictions of release curves by a model based on this desorption behavior have been successful in matching observed data.

## References


[1]M. Briec, F. Botter, J. J. Abassin, R. Benoit, P. Chenebault, M. Masson, B. Rausner, P. Sciers, H. Werle, and E. Roth, "In and Out-of-Pile Tritium Extraction From Samples of Lithium Aluminates," *J. Nucl. Mater.*, **141–143**, 357–363 (1986).

[2]P. C. Bertone, "The Kinetics that Govern The Release of Tritium from Neutron-Irradiated Lithium Oxide," *J. Nucl. Mater.*, **151**, 281–292 (1988).

[3]W. Breitung, H. Elbel, J. Lebkucher, G. Schumacher, and H. Werle, "Out-of-pile Tritium Extraction From Lithium Silicate," *J. Nucl. Mater.*, **155–157**, 507–512 (1988).

[4]T. Tanifuji, K. Noda, S. Nasu, and K. Uchida, "Tritium Release from Neutron-Irradiated $Li_2O$; Constant Rate Heating Measurements," *J. Nucl. Mater.*, **95**, 108–118 (1980).

[5]A. Skokan, D. Vollath, H. Wedemeyer, E. Gunther, and H. Werle, "Preparation, Phase Relationships and First Irradiation Results of Lithium Orthosilicate Doped with $Al^{+3}$ and $P^{+5}$ Ions," 15th Symp. on Fusion Technology, Utrecht, The Netherlands, Sept. 1988.

[6]V. Schauer and G. Schumacher, "Study of Adsorption and Desorption of Water on $Li_4SiO_4$," presented at STNM-7, Chicago, IL, Sept. 1988 (to be published in *J. Nucl. Mater.*).

[7]A. K. Fischer and C. E. Johnson, "Measurements of Adsorption in the $LiAlO_2$-$H_2O$(g) System," *Fusion Technology*, **15**, 1212–1216 (1989).

[8]J. B. Peri, "A Model for the Surface of $\gamma$-Alumina," *J. Phys. Chem.*, **69**, 220 (1965).

[9]M. Briec and E. Roth, "Tritium Extraction Mechanisms from Lithium Aluminates During In-Pile Irradiation Experiments," Proc. of Specialists' Workshop on Modelling Tritium Behavior in Fusion Blanket Ceramics, Chalk River, Canada, pp. 28–57 (1987).

[10]J. M. Miller, R. A. Verrall, D. S. MacDonald, and S. R. Bokwa, "The CRITIC Irradiation of $Li_2O$—Tritium Release and Measurement," presented at the Third Topical Meeting on Tritium Technology in Fission, Fusion and Isotopic Applications, Toronto, Canada, May 1988.

[11]J. P. Kopasz, S. W. Tam, and R. A. Verrall, "Modeling Unusual Tritium Release Behavior from $Li_2O$," *Fusion Technology*, **15**, 1217–1222 (1989).

[12]A. W. Smith and S. Aranoff, "Thermodesorption of Gases from Solids," *J. Phys. Chem.*, **62**, 684–686 (1958).

[13]D. A. King, "Thermal Desorption From Metal Surfaces: a Review," *Surf. Sci.*, **47**, 384–402 (1975).

[14]H. Kudo and K. Okuno, "Kinetic Studies of the Tritium Release Process in Neutron-Irradiated $Li_2O$ and LiOH," *J. Nucl. Mater.*, **101**, 38–43 (1981).

[15]J. Quanci, "Tritium Breeding and Release-Rate Kinetics from Neutron-Irradiated Lithium Oxide," Ph. D. Thesis, Dept. of Chemical Engineering, Princeton University, January 1989.




# Tritium Modeling of Experimental Results for Lithium-Metasilicate in the LISA-1 Experiment


GIANFRANCO FEDERICI, A. RENE RAFFRAY, AND MOHAMED A. ABDOU

Mechanical, Aerospace and Nuclear Engineering Department
University of California at Los Angeles
Los Angeles, CA



***A mathematical model and numerical method of calculation for tritium transport and release in a fine-grained ceramic were developed and applied to interpret results available from in situ or postirradiation annealing experiments in lithium-base breeder materials. The model treats the following transport path: (1) lattice diffusion from the grain interior to the grain edges, (2) migration along the grain boundaries, (3) adsorption and desorption on the breeder surface, and (4) interconnect porosity diffusion. At the present stage, particular emphasis has been given to the modeling of the bulk/pore interface where mechanisms such as adsorption from the bulk and from the pore and desorption to the pore are included. Initial results for tritium release calculations on lithium metasilicate ($Li_2SiO_3$) in the LISA-1[1] experiment are presented.***


## Introduction

A computer model has been developed with the aim to describe the complex tritium transport behavior in candidate ceramic breeder materials for fusion reactors. The main purpose of this analysis is to determine the influence of the controlling physical processes in the proposed transport sequence and to predict, with sufficient accuracy, the tritium release response and the concentration distributions as a function of different variables for a wide range of operating conditions. The model includes several individual transport mechanisms, adequately coupled, such as inter-granular diffusion, grain boundary diffusion, adsorption and desorption at the gas-solid interfaces, and diffusion along the interconnected porosity system. A new feature of the model is the detailed treatment of the complex phenomena that occur at the bulk/pore interface, which are believed to be crucial for tritium release calculations. To assess the predictive capability of the proposed model to reproduce the experimentally

observed release under steady state and transient conditions, a preliminary benchmark analysis has been carried out for the metasilicate sample P1 irradiated in the LISA-1[1] experiment. Initial results of this analysis are presented and the effect of several physical properties which potentially control the release kinetics are hereafter discussed.

## Modeling Development

### The Model Geometry

The model is based on the assumption of interconnected porosity in which the pores are represented as straight cylindrical capillaries having an effective radius $r_{ip}$ and length $L_e$. The unit cell in the model has been identified as the interconnected pore system and the cylindrical portion of the solid that surrounds it. In the present work the following expression for $L_e$ is used:[2]

$$(L_e/L)^2 = \tau$$

where L is the characteristic length and $\tau$ is the tortuosity factor, which, according to the model of Wakao and Smith,[3] is given by:

$$\tau = 1/\epsilon_p$$

where $\epsilon_p$ is the porosity of the material.

The pore radius $r_{ip}$ is given by the following expression[2]

$$r_{ip} = \frac{2\epsilon_p}{(S_{BET} \cdot \rho \cdot (1-\epsilon_p))}$$

where $\rho$ = solid breeder density (TD) ($Kg \cdot m^{-3}$); $S_{BET}$ = specific surface area ($m^2 \cdot Kg^{-1}$).

### Tritium-Transport Mechanisms Included in the Model

The proposed model provides for a multi-region calculation and includes several transport mechanisms, which are considered to be relevant to controlling physical processes for ceramic breeder materials. A schematic of the multiregion model is shown in Fig. 1. The tritium, after being generated from breeding reactions in the grain, diffuses (most likely in anionic form) to the grain edges and to the grain-boundary paths and reaches the bulk/pore interface where it



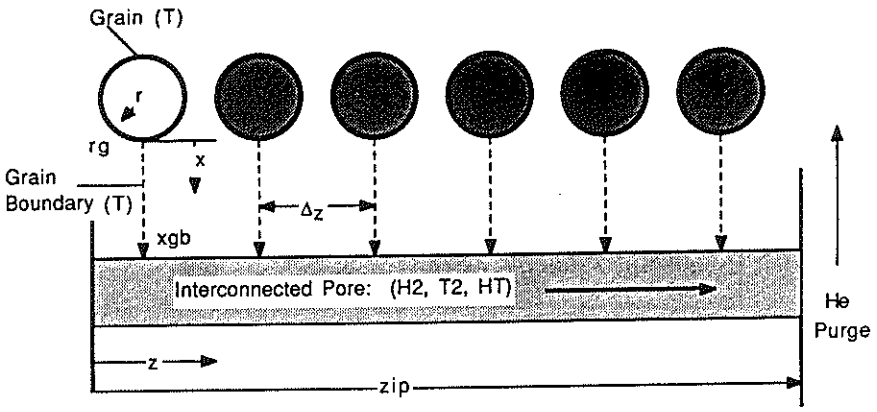


**Fig. 1. Schematic of the multi-region model.**

desorbs through the pores, most likely as molecules, in combination with any oxygen or hydrogen present at the surface. Tritium and tritium-bearing species then diffuse through the pores to the purge flow, where they are convected outside the solid breeder region. Therefore, surface phenomena, such as adsorption from the pore and from the bulk, desorption to the pore and eventually dissolution into the bulk, can play an important role in the overall tritium release kinetics and strongly influence the amount of gas which resides on the surfaces (expressed in terms of fractional coverage). Because of the complex nature of the mechanisms involved and the lack of basic experimental data, the characterization of the surface adsorption/desorption processes on lithium-based ceramics is very difficult. The modeling takes explicit account of the surface and its coupling with the interconnected pore and the bulk. Figure 2 shows a schematic diagram of the basic surface processes included in the model. The rate theory has been used to model the surface processes and the details of the scheme adopted are hereafter outlined.

### Formation of the Governing Equations

#### *Grain and Grain Boundary Regions*

The time-dependent diffusion equations for the tritium concentration within the grain and the grain boundary assuming spherical grains and slab-shaped grain boundaries can be written as follows:

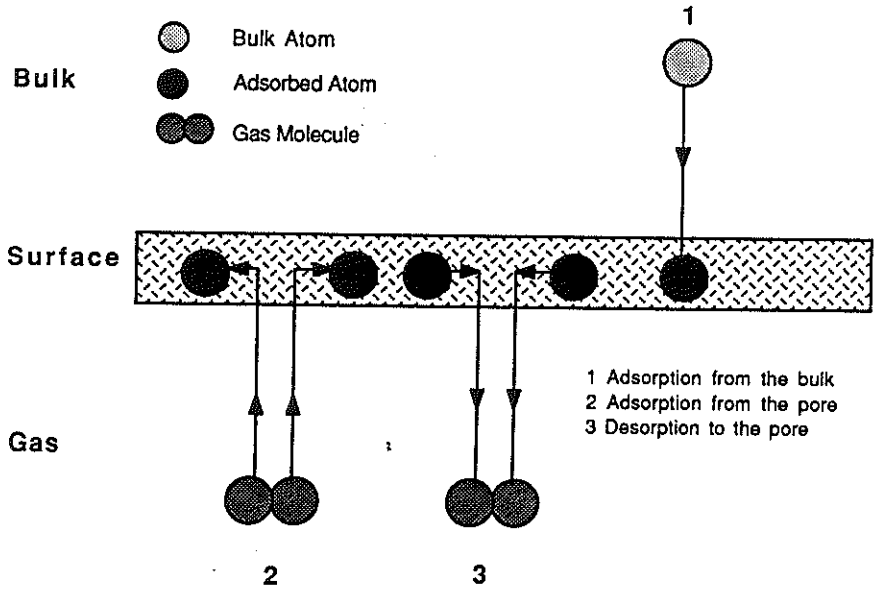


**Fig. 2. Schematic of the surface processes considered in the model.**

$$\frac{\partial C_g(r,t)}{\partial t} = D_g(T)\left[\frac{\partial^2 C_g(r,t)}{\partial r^2} + \frac{2}{r}\frac{\partial C_g(r,t)}{\partial r}\right] + G(r,t) \quad \text{for } 0 < r < a \text{ and for } t > 0 \tag{1}$$

$$\frac{\partial C_b(x,t)}{\partial t} = D_b(T)\left[\frac{\partial^2 C_b}{\partial x^2}(x,t)\right] \quad \text{for } 0 < x < b \text{ and for } t > 0 \tag{2}$$

where $C_g(r,t)$ = tritium concentration within the grain at spatial coordinate r and time t, (tritons•m$^{-3}$); $C_b(x,t)$ = tritium concentration within the grain boundary at spatial coordinate x and time t, (tritons•m$^{-3}$); $D_g(T)$, $D_b(T)$ = tritium diffusion coefficients as a function of the temperature T in the grain and grain boundary regions, respectively, (m$^2$•s$^{-1}$); $G(r,t)$ = volumetric tritium generation rate within the grain, (tritons•m$^{-3}$•s$^{-1}$); a, b = outer radius of the grain and length of the grain boundary path, respectively (m).



The applicable boundary, interface and initial conditions in conjunction with Eqs. (1) and (2) are

$$C_g(r = 0,t) = \text{finite} \tag{3}$$

$$C_g(r = a,t) = C_b(x = 0,t) \tag{4}$$

$$4\pi a^2 \cdot D_g(T)\left.\frac{\partial C_g}{\partial r}\right|_{r=a} = N_{gbg} \cdot A_{gb} \cdot D_b(T)\left.\frac{\partial C_b}{\partial x}\right|_{x=0} \tag{5}$$

$$A_{gb} \cdot D_b(T)\left.\frac{\partial C_b}{\partial x}\right|_{x=b} = R_{bulk}\, C_b\,(x=b,t)(1-\vartheta) \tag{6}$$

$$C_g(r,t=0) = C_{go}(r) \qquad \text{for } 0 \le r \le a \tag{7}$$

$$C_b(x,t=0) = C_{bo}(x) \qquad \text{for } 0 \le x \le b \tag{8}$$

In Eq. (5), $A_{gb}$ is the transversal area of the grain boundary path and $N_{gbg}$ is the effective number of one-dimension grain boundary paths associated with each grain. In Eq. (6), which couples the bulk region with the surface region, the term on the right represents the adsorption flux from the bulk. $R_{bulk}$ is the rate constant for adsorption from the bulk, $C_b(x = b,t)$ is the concentration in the grain boundary, just beneath the surface, and $(1 - \vartheta)$ represents the fraction of sites available for atoms coming from the bulk to be adsorbed on the surface. The right side of terms of Eqs. (7) and (8) are the initial tritium concentrations within the grain and grain boundary, respectively.

*Surface Region*

The three fluxes going to and from the surface shown in Fig. 2 are included in our surface model.[4] Balancing the adsorption fluxes from the pore and from the bulk with the desorption flux to the pore yields the following rate equation governing the coverage.

$$\frac{d[N_s \cdot \vartheta_j]}{dt} = R_{ads}(T)\ Cp^{(i)}(z,t)(1-\vartheta)^2 + R_{bulk}(T)C_b(x=b,t)(1-\vartheta) - R_{des}(T)\,\vartheta_j\,\vartheta \tag{9}$$

where $\vartheta_j$ = fractional coverage for the adsorbed species j (i.e., atomic fraction of tritium or hydrogen atoms on the surface); $\vartheta$ = total coverage = $\Sigma\,\vartheta_j$; $N_s$ = number of sites available ($\sim 10^{19}$ sites$\cdot$m$^{-2}$); $Cp^{(i)}$ (z,t) = concentration of species (i) along the pore at spatial coordinate z, and time t (molecules (i)$\cdot$m$^{-3}$) ((i) could represent either $H_2$, $T_2$, HT, or $H_2O$, $T_2O$, and HTO); and the rate constant can be expressed as follows:[4,5]

$$R(i)_{ads}(T) = \frac{\sigma}{\sqrt{8\times 10^{-3} M_{(i)}}}\ \sqrt{RT}\ \cdot \exp(-E_{ads/RT}) \tag{10}$$

$$R_{des}(T) = \upsilon_O N_s \exp(-E_{des/RT}) \tag{11}$$

$$R_{bulk}(T) = \beta_o \exp(-E_{\beta/RT}) \tag{12}$$

$E_{ads}$, $E_\beta$, and $E_{des}$ are activation energies, respectively, for adsorption from the pore and from the bulk and for desorption from the surface, and $\upsilon_o$ and $\beta_o$ are pre-exponential of the order of $1 \times 10^{13}$ s$^{-1}$.

***Interconnected Pore Region***

The pore is modeled as a straight cylinder and the governing 1-D diffusion equation can be written as follows for each tritium-bearing species.

$$\frac{\partial C_p^{(i)}(z,t)}{\partial t} = D_{Peff}^{(i)}(T)\frac{\partial^2 C_p^{(i)}(z,t)}{\partial z^2} + Sp^{(i)}(z,t) \tag{13}$$

where $D_{Peff}^{(i)}$ (T) = effective diffusion coefficient along the pore for species (i) (m$^2\cdot$s$^{-1}$); $Sp^{(i)}$ (z,t) = volumetric source rate within the pore (molecules (i)$\cdot$m$^{-3}\cdot$s$^{-1}$).

The boundary conditions for Eq. (13) are



$$\left.\frac{\partial Cp^{(i)}}{\partial z}\right|_{z=0} = 0 \tag{14}$$

(i.e. zero gradient at the beginning of the interconnected porosity system)

$$Cp^{(i)}\ (z = Le,t) = C_{P_o}^{(i)} \tag{15}$$

where in Eq. (15) $C_{P_o}^{(i)}$ represents the concentration of the species (i) gas in the purge stream, which is assumed known.

The source term in the pore diffusion equation couples the surface and the bulk with the interconnected pore system, and has to be expressed as the net rate of molecules leaving the surface at the solid/gas interface (i.e. desorption minus adsorption)

$$S_p^{(i)}(z,t) = (R_{des}(T)\,\vartheta_j\vartheta - R_{ads}(T)\Sigma\ Cp^{(i)}(z,t)(1-\vartheta)^2)\ \frac{S_{BET}\cdot\rho\cdot V_g\cdot N_{gip}}{V_{ip}} \tag{16}$$

where $V_{ip}$ is the volume of the interconnected porosity system and $N_{gip}$ is the number of grains associated with one interconnected porosity system.

At the present stage, the analysis was performed for LISA-1 cases with only tritium in the system, so that in the previous set of equations

$$\vartheta_j = \vartheta = \vartheta_T \tag{17}$$

$$C_p^{(i)} = C_{T_2} \tag{18}$$

The set of Eqs. (1) through (16) are solved numerically at each time step for each morphological breeder region (grain interior, grain boundary, surface, interconnected pore).

***Interconnected Pore Region***

$$D_{Peff}^{(i)} = \epsilon p^2\ Dp^{(i)} \tag{19}$$

$$Dp^{(i)} = \frac{1}{\frac{1-\alpha \cdot yi}{D_o^{(i)}} + \frac{1}{D_k^{(i)}}} \qquad (20)$$

and the Knudsen diffusivity $D_k$, which predominates when the characteristic length is of the order of the molecular mean free path, is given as:

$$D_k^{(i)}\ (m^2 \cdot s^{-1}) = 0.97\ r_{ip} \sqrt{\frac{T}{M_{(i)}}} \qquad (21)$$

for ordinary diffusion:

$$D_o^{(i)}\ (m^2 \cdot s^{-1}) = \frac{1.86 \times 10^{-7}\ T^3/2 \sqrt{\frac{1}{M_{(i)}} + \frac{1}{M_{He}}}}{P\sigma^2{}_i\ \Omega_i} \qquad (22)$$

$M_{(i)}$ = molecular weight for species i

$$\alpha = 1 - \sqrt{\frac{M_{(i)}}{M_{He}}}$$

$Y_{(i)}$ = fraction of species i; P = pressure in pore; $\sigma_i$, $\Omega_i$ are constants described in Ref. 6.

## Results of the Calculations and Discussion

To test the proposed model quantitatively against available experimental data, we have chosen as a part of an agreed benchmarking program to examine some of the observed results for the LISA-1[1] experiment. For this paper, a detailed analysis of the release from the sample P1 (lithium metasilicate) under temperature transients, in the region of 600°–685°C with pure helium as purge gas is reported. These calculations were made with the data given in Table I and II, and the results are shown in the next set of figures. Figure 3 shows the calculated normalized tritium release profile from the end of the interconnected porosity system for the metasilicate sample P1. The temperature transient and the observed release profiles are also indicated. The model reproduces with



**Table I. Geometrical Data, Material Properties and, Parameters Used in the Calculations (Corresponding to the LISA Experiment)**

| Geometric Data | |
|---|---|
| Grain radius, a (m) | $3.95 \times 10^{-5}$ |
| Grain boundary path length, b (m) | $2.21 \times 10^{-5}$ |
| Interconnected-porosity path length, L (m) | $1.0 \times 10^{-2}$ |
| Grain volume, $V_g(m^3)$ | $2.58 \times 10^{-13}$ |
| Pore radius $r_{ip}$ (m) | $2.47 \times 10^{-7}$ |

Material Properties and Data

| Purge Flow Characteristic | Solid Breeder $Li_2SiO_3$ (metasilicate) | |
|---|---|---|
| composition He | density (TD), $\rho$ ($Kg \cdot m^{-3}$) | $2.53 \times 10^3$ |
| pressure, P ($P_a$) $1.013 \times 10^5$ | porosity, $\epsilon_p$ (%) | 4 |
| | specific surface areas, $S_{BET}$ ($m^2 \cdot Kg^{-1}$) | 300/500/770 |
| | condensation coefficient[5], $\sigma$ | 0.4 |
| | tritium gener. rate, G ($tritons \cdot m^{-3} \cdot s^{-1}$) | $8.5 \times 10^{18}$ |

| Grain Region | Grain Boundary Region |
|---|---|
| $D_g(T) = D_{go} \exp E_{dg}/(RT)$ | $D_b(T) = D_{bo} \exp(-E_{db/(RT)})$ |
| $D_{go}(m^2 \cdot s^{-1}) = 7.9 \times 10^{-10}$[8] | Grain boundary diffusion is believed to be faster than bulk diffusion and $D_b$ is set here as being $10^5 \times D_g$. |
| $E_{dg}(KJ \cdot mol^{-1}) = 77.4$[8] | |

**Table II. Heat of Adsorption as a Function of the Coverage for $H_2O(g)$-$LiAlO_2$ System. Data from Fischer et al.[7]**

| $\vartheta$ | $\vartheta$ ($KJ \cdot mol^{-1}$) |
|---|---|
| 0.001 | $3.6 \times 10^2$ |
| 0.00316 | $2.9 \times 10^2$ |
| 0.01 | $2.2 \times 10^2$ |
| 0.0316 | $1.5 \times 10^2$ |
| 0.1 | $0.8 \times 10^2$ |

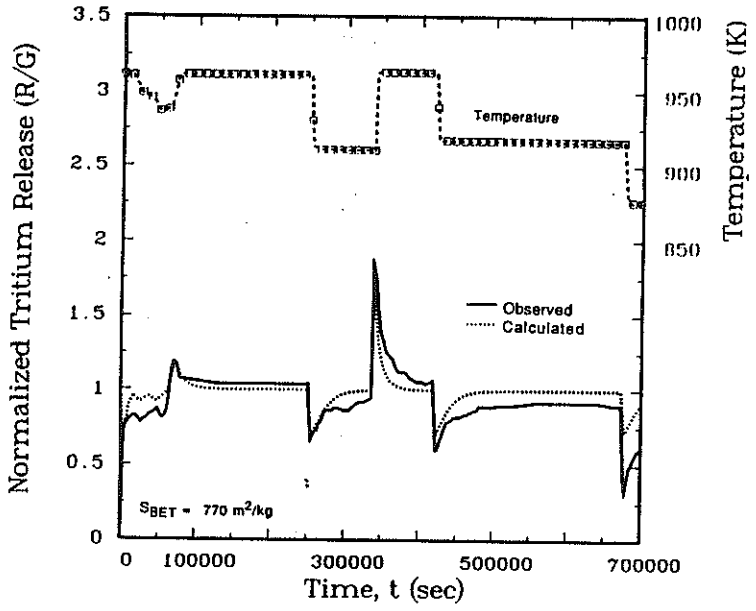


**Fig. 3. Calculated and observed normalized tritium release from sample P1 (metasilicate).**

reasonably good accuracy the observed release profile and predicts quite well both the magnitude of the peaks and dips, produced by the corresponding temperature transients, and the slope of the profile which represents the rate of change of the release.

Previous modeling studies on the behavior of tritium transport during temperature transient conditions[9,10] resulted in the identification of the ceramic breeder microstructure (e.g., grain size, pore size), the desorption activation energy, and the transient scenario as important factors affecting the release response. In this study the effects of the following key variables on the kinetics of the release, as well as on its relative magnitude, were investigated: (1) effect of the specific surface area, (2) effect of the desorption activation energy from the breeder surface, (3) effect of the diffusion activation energy within the grain, and (4) effect of gas diffusivity along the interconnected porosity system. Because of computing-time constraints, the proposed parametric analyses were carried out over about half the total time interval shown in Fig. 3, precisely between 69.4 and 152.8 hrs, where effects due to both increase and decrease in temperature are contained.



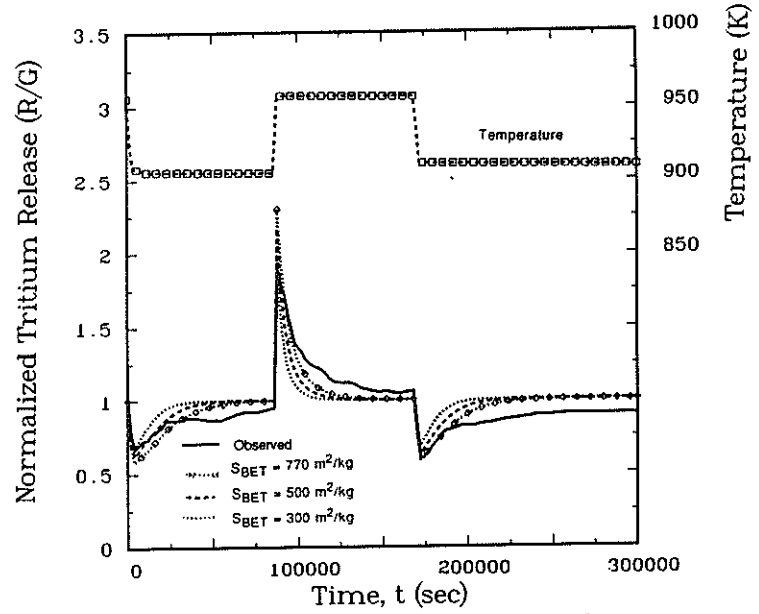


**Fig. 4. Effect of the specific surface area on tritium release.**

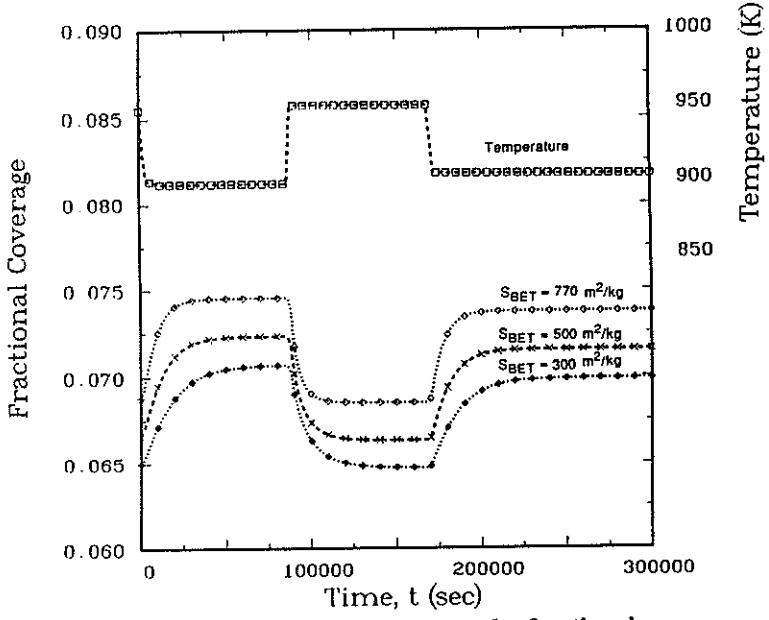


**Fig. 5. Effect of the specific surface area on the fractional coverage.**

In order to show the effect of the solid breeder specific surface area ($S_{BET}$) on tritium release response, a parametric analysis was carried out for three different values of $S_{BET}$ ((1) 300, (2) 500, (3) 770 $m^2 \cdot k_g^{-1}$). The last value is given as reference for the orthosilicate.[11] The resulting effect on tritium release is shown in Fig. 4. The best with the experimental profile is obtained for a value of $S_{BET}$ = 770 $m^2 \cdot k_g^{-1}$, which was also used in Fig. 3. The profiles in Fig. 5 show the influence of the specific surface area on the tritium coverage. These results confirm the importance of the surface region, which acts like a valve and controls the rate of both filling of gas from the bulk and from the pore, as well as the desorption flux to the pore. Furthermore, to show how the magnitude of the activation energy for the desorption process may affect the overall release kinetics a parametric analysis was also performed for three different values of the heat of adsorption. In our model, estimates of the activation energy for desorption have been made from values of heat of adsorption as a function of the coverage available for the $H_2O(g)$-$LiAlO_2$ system,[7] on the basis that the activation energy for desorption is equal to the sum of the heat of adsorption and the activation energy for adsorption. The heat of adsorption data are used here as an approximation because of the lack of data for the desorption activation energy as a function of coverage for lithium ceramics and hydrogen or water, whose experimental determination is again recommended here.[9] In the calculations a constant value of 50 KJ/mol for the adsorption activation energy from the pore and 20 KJ/mol for adsorption from the bulk were used following the assumption that the adsorption activation energies are low. Changes of 10–20% in these values were found to weakly affect the results. The value resulting from the following formula for the desorption activation energy was used.

$$E_{des}(\vartheta) = E_{ads} + f \times Q\ (\vartheta) \qquad (23)$$

where Q ($\vartheta$) is the heat of adsorption as a function of the coverage shown in Table II and $f$ is a factor, which was set respectively, for the three cases investigated, equal to 0.5, 1, and 1.2. Results of this parametric analysis for both tritium release and coverage are shown in Figs. 6 and 7. As expected, the coverage is substantially affected by changes in the desorption activation energy. The tritium release transients are markedly lower for the case with lowest desorption activation energy as a result of the coverage being ten times lower than for the reference case. However the tritium release behavior is not as influenced for the case with the highest activation energy since the increase of coverage, as compared to the reference case, is only about a factor of 1.5. Figures 8 and 9 show the effect of a change in the interconnected pore diffusion



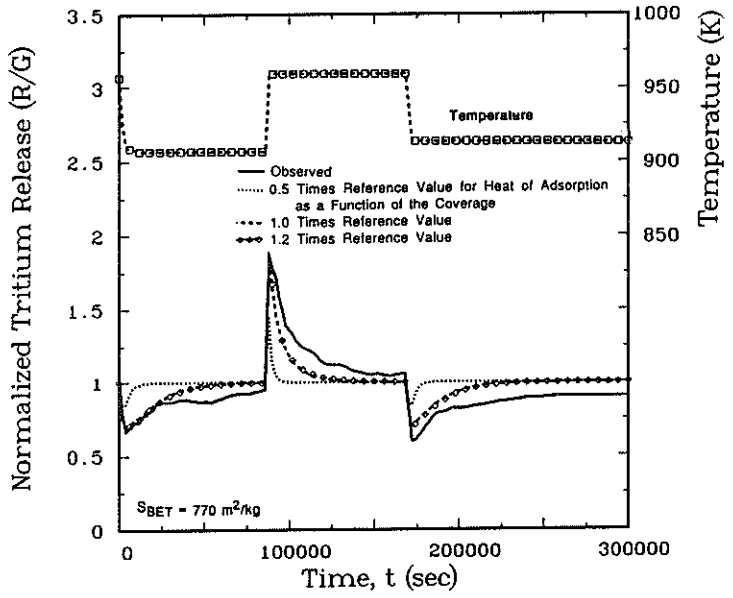


**Fig. 6. Effect of the activation energy for desorption on tritium release.**

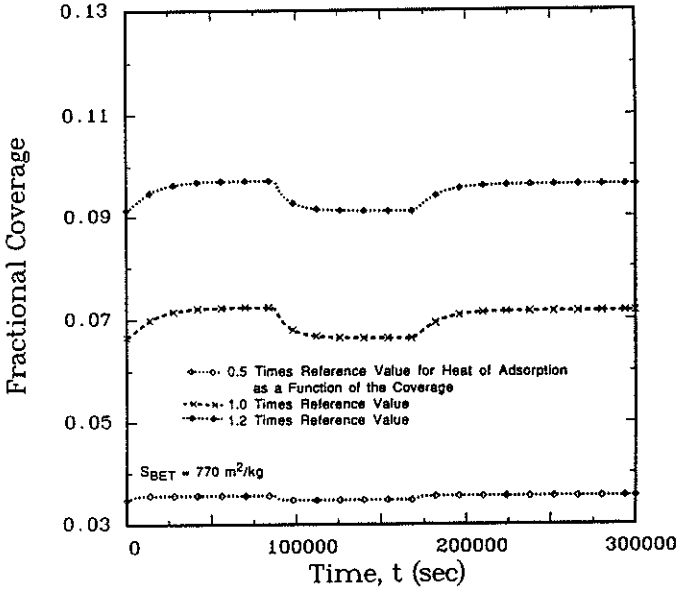


**Fig. 7. Effect of the activation energy for desorption on the fractional coverage.**

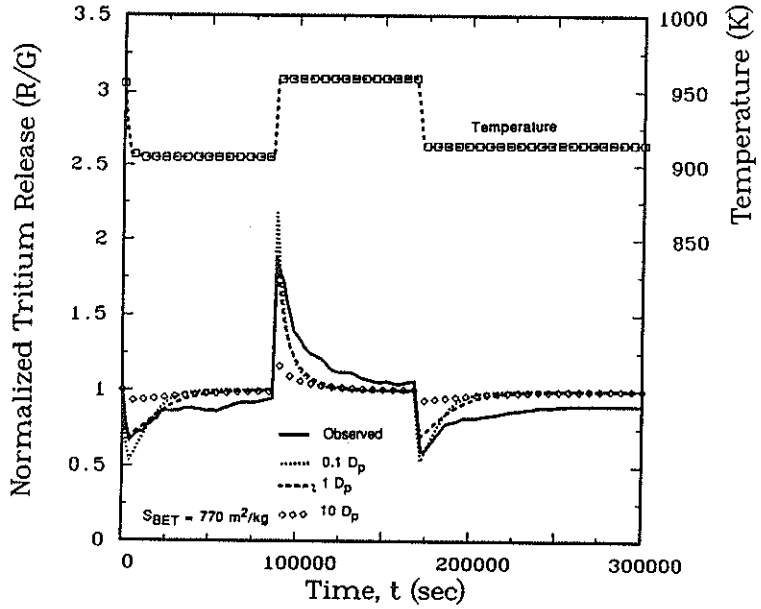


**Fig. 8. Effect of the pore diffusion coefficient on tritium release.**

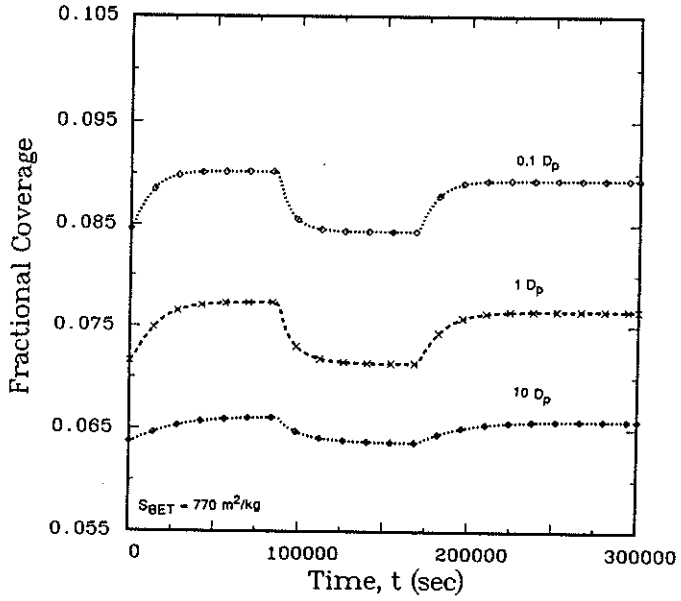


**Fig. 9. Effect of the pore diffusion coefficient on the fractional coverage.**



coefficient on the tritium release from the end of the interconnected pore system and the surface coverage. Three cases were investigated; (1) the value of $Dp_{eff}$ given by Eq. (19); (2) $0.1 \times Dp_{eff}$; (3) $10 \times Dp_{eff}$. The pore diffusion coefficient strongly affects the release response and the effect on the tritium release peak is quite marked. For fast diffusion in the pore ($10\ Dp_{eff}$), the tritium concentration in the pore is low and the resulting coverage is also low. Thus, temperature transients for that case have a lower effect on the tritium release. For slow diffusion in the pore ($0.1\ Dp_{eff}$), the reverse occurs and the tritium release is markedly affected by temperature transients. This could represent a case where sintering would have significantly closed the pores and effectively slowed down the pore diffusion. Finally, an analysis was performed by changing the value of the activation energy for diffusion within the grain. No relevant changes in the tritium release response were observed, showing that, as inferred by the above analysis, the tritium release behavior is not diffusion controlled, but surface controlled for the case with no hydrogen in the helium purge.

## Summary

A comprehensive model for predicting transient tritium behavior in lithium-based ceramic materials has been developed. It represents an attempt to develop a computer code with an efficient predictive capability to describe the tritium transport and release kinetics as a function of different variables and for a wide range of operating conditions. The model follows the basic physics of the expected transport process sequence, and particular emphasis is given to the analysis of surface phenomena, such as gas adsorption and desorption, which seem to play a crucial role for the accurate prediction of the release kinetics and gas concentration distributions. It is important for a code to properly describe the underlying physics, since fits obtained with physically unsound models to experimental data by varying suitable effective parameters, will fail whenever extrapolations are needed to new ranges of operating conditions. The model was developed so as to include the capability of analyzing temperature and purge flow chemistry transients. In this paper, the following key issues are addressed in conjunction with the analysis of the metasilicate sample P1 irradiated in the LISA-1 experiment: (1) identification of the transport steps relevant to reproduce the experimental tritium release profile and (2) identification of the key parameters which affect the release kinetics. The most important results from the application of the model for a temperature change under the condition of pure helium purge flow are the sensitivity of the tritium release behavior to crucial factors such as specific surface area, desorption activation energy, and pore diffusivity, which all influence the dynamics of tritium adsorption and desorption and determine the amount of tritium which resides on the surfaces.

This strongly indicates that tritium release is surface controlled in this case. It then becomes important to experimentally determine the values of the activation energies for adsorption and desorption as a function of the coverage for both the lithium ceramic/hydrogen and lithium ceramic/water cases. Future applications of the model will include analysis of experimental results for temperature transients with hydrogen in the purge and purge flow chemistry transients.

## Acknowledgement

This work was performed under U.S. Department of Energy Contract DE-FG03-86ER52123.

## References

[1]H. Werle, J. J. Abassin, M. Briec, R. G. Clemmer, H. Elbel, H. E. Hafner, M. Masson, P. Sciers, and H. Wedemeyer, "The LISA-1 Experiment: In-Situ Tritium Release Investigations," *J. Nucl. Mater.*, 141-143, 321-326, (1986).

[2]G. R. Youngquist, "Diffusion and Flow of Gases in Porous Solids," *Ind. Eng. Chem.*, 62[8], 52-63, (1970).

[3]N. Wakao and J. M. Smith, "Diffusion in Catalyst Pellets," *Chem. Eng. Sci.*, 17, 825-834, (1962).

[4]M. A. Pick and K. Sonnemberg, "A Model for Atomic Hydrogen—Metal Interactions—Application to Recycling, Recombination and Permeation," *J. Nucl. Mater.*, 131, 208-220, (1985).

[5]D. O. Hayward and B. M. W. Trapnell, "Chemisorption," 2nd ed. Butterworth, London (1964).

[6]J. M. Smith, "Chemical Engineering Kinetics"; Chemical Engineering Series, third edition McGraw-Hill (1981).

[7]A. K. Fischer and C. E. Johnson, "Measurements of Adsorption in the $H_2O(g)$-$LiAlO_2$ System," *Fusion Technology*, 15, [2], 1212-1216, (1988).

[8]K. Okuno and H. Kudo, "Tritium Diffusivity in Lithium-Based Ceramic Breeders Irradiated with Neutrons," presented at the International Symposium on Nuclear Technology, Tokyo 10-19 April 1988.

[9]J. P. Kopasz and C. E. Johnson, "Modeling of Tritium Transport in Ceramic Breeder Materials"; Semiannual Progress Report on Fusion Reactor Materials, DOE/ER-0313/4, 287-288 (3/1988).

[10]A. R. Raffray, M. A. Abdou, P. J. Gierszewski, "Modeling of Tritium Behavior in Solid Breeders", presented at the Symposium on Fabrication and Properties of Lithium Ceramics, American Ceramic Society, Pittsburgh, PA, (April 1987).

[11]H. Werle, W. Breitung, M. Briec, R. G. Clemmer, H. Elbel, H. E. Hafner, M. Masson, G. Schumacher, and H. Wedemeyer, "The LISA-2 Experiment: In-Situ Tritium Release from Lithium Orthosilicate ($Li_4SiO_4$)," *J. Nucl. Mater.*, 155-157, 538-543, (1988).



# Hydrogen-Tritium Exchange on the Surface of Ceramic Breeders

SATORU TANAKA, NAOSHI SUZUKI, KENJI YAMAGUCHI, AND MICHI YAMAWAKI

Nuclear Engineering Research Laboratory
University of Tokyo
2-22, Shirakata, Tokai-mura
Ibaraki, Japan 319-11

*Exchange reactions of hydrogen isotopes on the surface of $Li_2O$ and $LiAlO_2$ w experimentally studied. At first, the breeder was loaded with tritiated water vap Then, adsorbed HTO was desorbed with He + $H_2$ (10-10000 vppm) sweep g Chemical forms of desorbed tritium were HT and HTO, and the fraction of HT found to become larger for higher $H_2$ concentration. Reaction rate for HT release found to be proportional to the amount of residual tritium and to the square roo hydrogen concentration in the sweep gas. This infers that dissociation of hydro occurs on the surface.*

## Introduction

One of the major issues in developing a fusion reactor system is that tritiu production must be self-sustaining. Tritium must be generated in sufficic quantities in high TBR and must be recovered in a short time. Short ti means short tritium residence time and this corresponds to low tritium inventc in the blanket. In order to estimate the tritium inventory with good accura the tritium migration processes must be fully understood. However, until no surface reaction—desorption and/or exchange reaction—on the solid breedi material has not been extensively studied, although it may sometimes cause major fraction for tritium inventory in the blanket. In this connection, we ha been studying surface reactions by several methods. By in situ tritium relea experiments (TTTEx) at the University of Tokyo, the released chemical form tritium and the residence time were found to be strongly influenced by tl chemical composition of the sweep gas.[1-3] When hydrogen gas was added to tl helium sweep gas, the fraction of HT in the sweep gas increased with l